URSI GASS 2021, Rome, Italy, 28 August - 4 September 2021

Radiometer Design for the REACH 21cm Global Experiment

Nima Razavi-Ghods*(1), Ian Roque(1), and Will Handley(1)(2)
(1) Astrophysics Group, Cavendish Laboratory, JJ Thomson Avenue, Cambridge, CB3 0HE, UK
(2) Kavli Institute for Cosmology, Madingley Road, Cambridge, CB3 0HA, UK

Abstract

Detecting signals from the Cosmic Dawn using "global" experiments requires an unprecedented level of instrumental calibration, especially to remove possible systematics which arise from the interaction between the antenna and receiving systems. In this paper we describe the calibration methods which can be applied to a range of experiments including the Radio Experiment for the Analysis of Cosmic Hydrogen (REACH) which is an instrument being designed to detect such signals. We use the functions described by noise wave parameters in a fast Bayesian pipeline to determine physical calibration coefficients which can describe the systematics. This approach when used in the field and on the fly could calibrate the absolute temperature measured by the antenna down to sub-kelvin levels. In this paper we present the Bayesian framework and simulated results of our pipeline using models derived from early laboratory measurements. A major advantage of this approach is that we can properly model the uncertainties in our measurement system.

1 Introduction

Over the past decades, radio experiments have been designed to measure the impact on the hyperfine 21-cm line of neutral hydrogen in the intergalactic medium (IGM) arising from X-ray and UV emission from the first bright objects [1]. The flip in the magnetic moments of the proton and electron in the hydrogen atom from a higher to lower energy state results in weak radiation at a rest wavelength of 21-cm (1420 MHz). The expansion of the Universe redshifts these photons from earlier epochs to lower observed frequencies of 50-200 MHz. This signal is therefore a powerful probe for exploring the formation of the first objects in the Universe which heat/couple to the IGM and impact the gas spin temperature. A model for the sky-averaged or global brightness temperature of this signal is given by

$$T_B = 27x_{HI}\left(\frac{1+z}{10}\right)^{1/2}\left[1-\frac{T_{CMB}}{T_S}\right] \tag{1}$$

where z is the redshift, x_{HI} is the fraction of neutral hydrogen in the IGM and T_{CMB} and T_S are the CMB and gas spin temperature, respectively. The ratio between the gas spin temperature and the CMB which serves as a backlight can produce either absorption or emission in the brightness temperature.

In early 2018, the Experiment to Detect the Global EoR Signature (EDGES) reported a detection [2] of this signal centred at 78 MHz having a width corresponding to a period between 180-270 million years after the Big Bang. The result from the EDGES experiment showed an absorption depth of $\sim 0.5K$, which was a factor of two greater than the largest predictions from theoretical models. This discrepancy would suggest that the IGM was much cooler than previously thought and would require new physics such as dark matter interactions that cool the IGM or excess radio backgrounds to explain the difference. Several follow up experiments including REACH [3] are aiming to make an independent detection of this signal.

Observing a weak 21-cm signal in presence of bright foregrounds which are several orders of magnitude larger is a major challenge for many instruments, none more so that those designed to measure the global monopole signal. In order to develop such an instrument, several key factors must be observed. The instrument should be designed to have fairly low chromaticity (although this can never be perfect), it should have good models which can be used to describe how the antenna beam couples to the sky and the entire receiver and antenna mismatch should be calibrated to achieve absolute antenna temperature down to millikelvin levels. This paper focuses on the progress made regarding the latter, using a method developed by the EDGES team and improved upon using our Bayesian framework.

2 Radiometer Design

The primary job of a radiometer is to effectively "model" the observing system using additional sources, such that the systematic instrument response can be calibrated out. For the aforementioned global 21cm experiments, the observing system is conceptually very simple. It consists of a broadband antenna, a receiver which contains a low-noise amplifier (LNA) at the very front end and a readout system. Calibrating these systems can range from the very simple Dicke switching [4] to the more elaborate noise wave characterisation which aims to properly model the interaction between the antenna and the receiver. Given our objective is to design a system which can achieve mK calibration, we follow the noise waves formalism which has been used by EDGES [5, 6] and relies on information being gathered from each of those blocks in the system including the antenna reflection coefficient.

Firstly using a Dicke switch [4], we measure two reference standards; an ambient load and a noise source, in addition to a series of external calibration sources attached to the receiver input in lieu of the antenna. These include a 'cold' load, a 'hot' load heated to ≈ 380 K, and various "cable" standards which include but are not limited to an open-ended cable and a shorted cable.

When taking measurements, reflection coefficients of the source (Γ_{source}) and the receiver (Γ_{rec}) are taken as well as power spectral densities (PSDs) of the calibration sources (P_{source}), the reference load (P_{L}) and the reference noise source (P_{NS}) [6]. These measurements are used to calculate a preliminary 'uncalibrated' antenna temperature T^{*}_{source}

$$T^{*}_{\text{source}} = T_{\text{NS}} \left(\frac{P_{\text{source}} - P_{\text{L}}}{P_{\text{NS}} - P_{\text{L}}} \right) + T_{\text{L}}, \tag{2}$$

where T_{L} and T_{NS} are assumptions for the noise temperatures of the reference load and noise source, respectively. This quotient is used to calibrate out any time-dependent system gain that emerges from a series of filters, amplifiers and cables, as well as the analogue-to-digital converter (ADC) within the experimental setup. Each PSD measurement can be expressed in terms of specific contributions from the reflection coefficients of the receiver as well as the source under test which can include the antenna. A set of "noise wave" functions are then used to describe the reflections from the antenna input back into the receiver. One term (T_{unc}) is used to described noise which is uncorrelated with the LNA temperature and two terms, T_{sin} and T_{cos} are used to described the sin and cosine components of the correlated noise. These contributions are detailed in [6]. When expanding Equation 2 using these specific contributions, we obtain a linear relationship between the uncalibrated input temperature and a final calibrated temperature of any source connected to the receiver input. This is defined by

$$\begin{aligned} T_{\text{NS}} \left(\frac{P_{\text{source}} - P_{\text{L}}}{P_{\text{NS}} - P_{\text{L}}} \right) + T_{\text{L}} = T_{\text{source}} & \left[\frac{1 - |\Gamma_{\text{source}}|^2}{|1 - \Gamma_{\text{source}} \Gamma_{\text{rec}}|^2} \right] \\ + T_{\text{unc}} & \left[\frac{|\Gamma_{\text{source}}|^2}{|1 - \Gamma_{\text{source}} \Gamma_{\text{rec}}|^2} \right] \\ + T_{\text{cos}} & \left[\frac{\operatorname{Re}\left(\frac{\Gamma_{\text{source}}}{1 - \Gamma_{\text{source}} \Gamma_{\text{rec}}} \right)}{\sqrt{1 - |\Gamma_{\text{rec}}|^2}} \right] \\ + T_{\text{sin}} & \left[\frac{\operatorname{Im}\left(\frac{\Gamma_{\text{source}}}{1 - \Gamma_{\text{source}} \Gamma_{\text{rec}}} \right)}{\sqrt{1 - |\Gamma_{\text{rec}}|^2}} \right], \end{aligned} \tag{3}$$

where all parameters are frequency-dependent. Therefore in order to estimate of the noise wave parameters, T_{source}, Γ_{source} and Γ_{rec} are measured along with the PSDs as often as required.

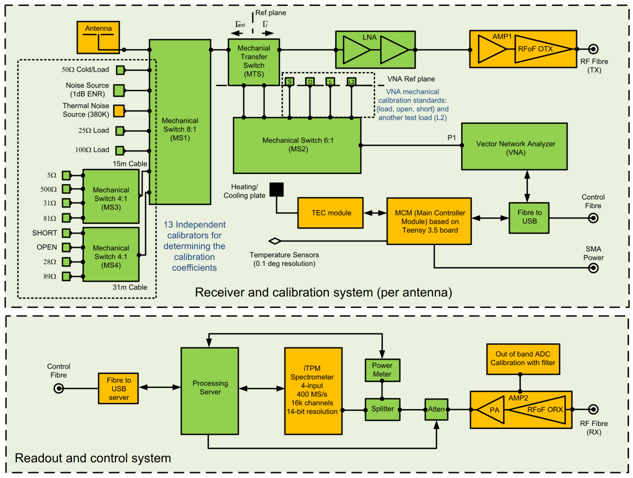

Figure 1. REACH radiometer design

Using this technique we have devised a receiver and calibration system for the REACH global 21-cm experiment shown in Figure 1.

The instrument consists of a field unit located at the antenna which incorporates a number of electro-mechanical switches to switch in both the reference and the calibration sources. These switches have very low loss (typically 0.01dB in this band) and an isolation of over 100dB. The field unit is being designed to be fully autonomous requiring no physical interaction once installed. The switches which include a transfer switch allow a vector network analyser (VNA) to measure the reflection coefficients of the sources and the LNA. An on-board micro-controller facilitates this process along with controlling the environmental temperature. All signals (control and RF) are transported via RF-over-fibre cables to avoid interference and extra loss to a readout system which converts signals back into RF and digitises them using a 400 Msps 14-bit spectrometer with 16k channels in the DC-200MHz band. The calibration sources used offer strategic sampling of the noise waves as a function of impedance and go much further than a standard open or shorted cable. A plot of this is shown in Figure 2 along with a typical dipole antenna impedance in the 60-120MHz band. This allows better sampling and ultimately can give a more accurate calibration solution for T_{unc}, T_{sin} and T_{cos}.

3 Bayesian method

It is desirable to be able to compute the calibration coefficients described in Equation 3 using a Bayesian approach which has a number of key advantages over a standard least squares fit. Firstly, it is easy to incorporate more or fewer sources into our pipeline, we can compute coefficients very quickly on the fly and can understand the correlation between these parameters not to mention have a better handle

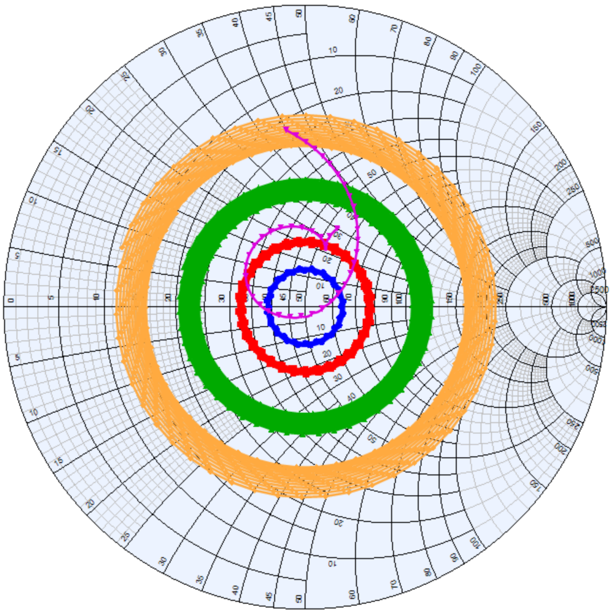

Figure 2. A smith chart showing example sources being used for REACH compared to a typical dipole antenna. Each colour represents a pair of cable sources as a function of frequency.

on how uncertainties in our measurement propagate down the line. This approach especially lends itself well to methods where some joint estimation of parameters including astrophysical terms can be determined. If there is some bias in one of the calibrators, we can easily determine which and potentially remove that data from our final solution. We start by writing Equation 3 as

$$T_{\mathrm{source}} = X_{\mathrm{unc}}T_{\mathrm{unc}} + X_{\cos}T_{\cos} + X_{\sin}T_{\sin} + X_{\mathrm{NS}}T_{\mathrm{NS}} + X_{\mathrm{L}}T_{\mathrm{L}} \tag{4}$$

In this equation, there are no squared or higher-order terms, allowing us to take advantage of the linear form by grouping the data and noise wave parameters into separate matrices

$$\begin{aligned}\mathbf{X} &\equiv \begin{pmatrix} X_{\mathrm{unc}} & X_{\cos} & X_{\sin} & X_{\mathrm{NS}} & X_{\mathrm{L}} \end{pmatrix}^{\top},\\ \Theta &\equiv \begin{pmatrix} T_{\mathrm{unc}} & T_{\cos} & T_{\sin} & T_{\mathrm{NS}} & T_{\mathrm{L}} \end{pmatrix}^{\top}.\end{aligned} \tag{5}$$

Here, all of our data; the reflection coefficient measurements and power spectral densities, are grouped in a frequency-dependent $\mathbf{X}$ vector which forms a matrix where one of the axes is frequency. The calibration parameters are collected into a Θ vector which serves as our model. Applying of these definitions condenses the calibration equation into

$$y \equiv T_{\mathrm{source}} = \mathbf{X}^{\top}\Theta + \sigma, \tag{6}$$

with the noise vector σ representing our error and y being our notation for independent observations on T_{source}. Since EDGES assumes that each power spectral density measurement is frequency independent, we have assumed that σ

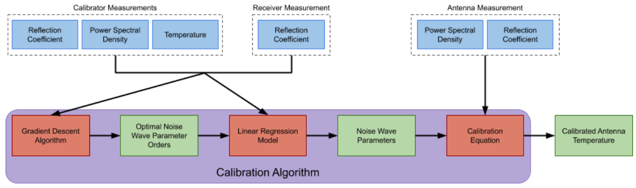

Figure 3. Outline of the calibration algorithm. Blue blocks represent data to be taken, red blocks represent calculations and green blocks represent outputs.

is a multivariate normal distribution. This assumption is implicit in the EDGES analysis in which they use a least-squares minimisation approach for solving model parameters.

For calibration of the receiver, we are concerned with the construction of predictive models of the noise wave parameters, Θ, in the context of some dataset, y. We can use Θ to calculate the probability of observing the data given a specific set of noise wave parameters:

$$p\left(y|\Theta,\sigma^2\right) = \frac{1}{\left(2\pi\sigma^2\right)^{N/2}} \exp\left\{-\frac{1}{2\sigma^2}\left(y - \mathbf{X}\Theta\right)^{\top}\left(y - \mathbf{X}\Theta\right)\right\} \tag{7}$$

This distribution on the data is the *likelihood*. Our model must also specify a *prior* distribution, quantifying our initial assumptions on the values and spread of our noise wave parameters which we specify as a normal inverse gamma distribution [7]. The likelihood in Equation 7 is determined by a set of values for our model Θ. We can marginalise out the dependence on Θ and our noise term by integrating over the prior distribution by both Θ and σ^2 at once. With the prior distribution specified and using the *evidence*, which gives the probability of observing the data y given our model, we can use Bayes' equation to invert the conditioning of the likelihood and find the *posterior* using the likelihood, prior and evidence [7]

$$p\left(\Theta,\sigma^2|y\right) = \frac{p\left(y|\Theta,\sigma^2\right)p\left(\Theta,\sigma^2\right)}{p\left(y\right)}. \tag{8}$$

The application of conjugate priors within our methodology enables our algorithm to be many orders of magnitude faster than techniques that use full numerical sampling via MCMC methods over many parameters. This allows for an in-place calibration with the data acquisition instead of relying on off-site measurements. We use polynomials to model the individual noise waves, although other functions can be used. Each of these parameters are optimised using a gradient descent algorithm rather than applying a blanket multi-order term to all noise wave parameters. A schematic of the calibration algorithm is shown in Figure 3.

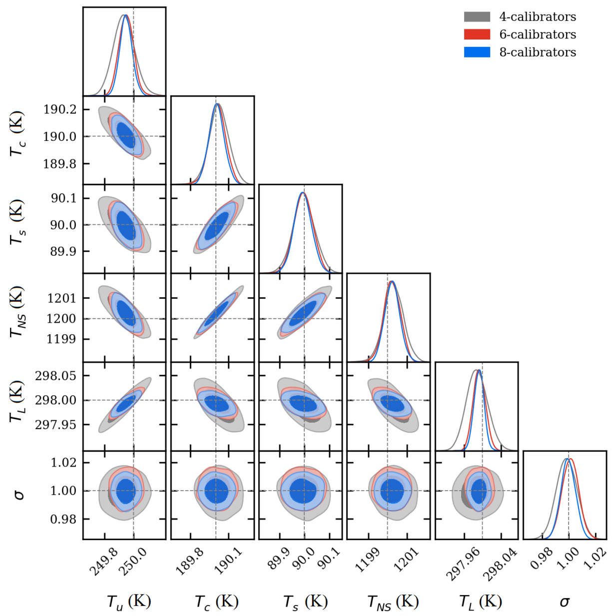

Figure 4. Posterior results of our pipeline using data from four, six and eight calibrators shown in grey, red and blue, respectively. Cross hairs mark the values of noise wave parameters used to generate the data.

4 Results

By carrying out a number of laboratory measurements of the reflection coefficients of real sources described in Figure 1, we could obtain a set of mock PSD to determine the functionality of our pipeline before deploying on the actual radiometer hardware. This also allows us to incorporate a model for noise in two places independently, one for the reflection coefficients and the other for the PSDs. Using up to eight calibrators, we can see the posterior results shown in Figure 4. As shown, the inclusion of more calibrators increases the constraint on the resulting noise wave parameters. The values of noise wave parameters used to generate the data as indicated by the cross hairs in 4 all fall within statistical consistency of our pipeline's resulting posterior averages for models using all eight calibrators.

When this calibration model is used to calibrate an ambient-temperature 50Ω load, the RMS error between the calibrated temperature and the measured temperature is 8 mK, well within the 1σ noise level (bottom right panel of 5).

5 Conclusions

In this paper we have described a robust radiometer suited for global 21cm monopole experiments. We have described the calibration process and the type of system we would like to employ in the field for the REACH experiment. Using a Bayesian framework with the aid of conjugate priors we are able to determine calibration coefficients quickly. We have demonstrated our pipeline using a set of mock data derived from laboratory measurements of source reflection coefficients. Using a realistic noise model, we can determine the output temperature to a high level of accuracy.

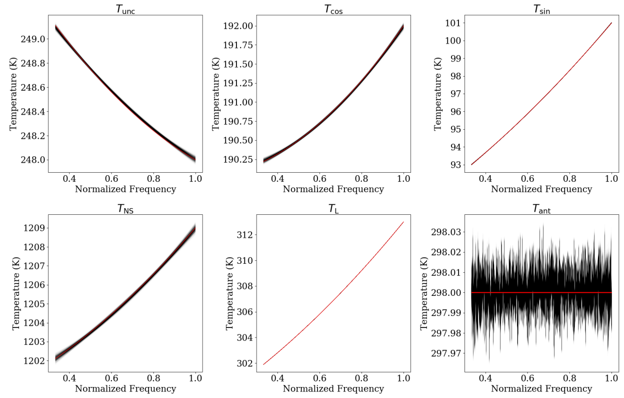

Figure 5. Results from 1000 samples using data generated with our more realistic noise model (shown in black). The second-order noise wave parameters shown in red are used to generate the data inputted to our pipeline. This solution is applied to an ambient-temperature load in the bottom right panel.

References

[1] Jonathan R. Pritchard and Abraham Loeb. 21 cm cosmology in the 21st century. *Reports on Progress in Physics*, 75, July 2012.

[2] Judd D. Bowman, Alan E. E. Rogers, Raul A. Monsalve, Thomas J. Mozdzen, and Nivedita Mahesh. An absorption profile centred at 78 megahertz in the sky-averaged spectrum. *Nature*, 555(7694):67–70, March 2018.

[3] Eloy de Lera Acedo. Reach: Radio experiment for the analysis of cosmic hydrogen. in preparation, 2019.

[4] R. H Dicke. The measurement of thermal radiation at microwave frequencies. *Review of Scientific Instruments*, 17(268), 1946.

[5] R. P. Meys. A wave approach to the noise properties of linear microwave devices. *IEEE Transactions on Microwave Theory and Techniques*, MTT-26:34–37, 1978.

[6] Raul A. Monsalve, Alan E. E. Rogers, Judd D. Bowman, and Thomas J. Mozdzen. Calibration of the edges high-band receiver to observe the global 21 cm signature from the epoch of reionization. *The Astrophysical Journal*, 835(1):49, January 2017.

[7] Ian L. V. Roque, Will J. Handley, and A. Razavi-Ghods. Bayesian noise wave calibration for 21-cm global experiments. in press, 2021.